HEAT VENTILATION EFFICIENCY OF URBAN SURFACES USING LARGE-EDDY SIMULATION

M. Cristina L. CASTILLO[1], Manabu KANDA[2], Marcus Oliver LETZEL[3]

[1]Member of JSCE, Doctoral Student, Dept. of International Development Engineering, Tokyo Institute of Technology (2-12-1 Ookayama, Meguro-ku, Tokyo 152-8552, Japan)

[2]Member of JSCE, Dr. of Eng., Associate Professor, Dept. of International Development Engineering, Tokyo Institute of Technology (2-12-1 Ookayama, Meguro-ku, Tokyo 152-8552, Japan)

[3]Dr. of Natural Sciences, Institute of Meteorology and Climatology, University of Hannover (Herrehäuser Str. 2, 30419 Hannover, Germany)

Heat ventilation of various urban surfaces with uniform heating were numerically measured via bulk transfer coefficients. A parallelized Large-Eddy Simulation Model (PALM) was used to simulate a 1-m/s wind over explicitly resolved cube arrays of 24-m buildings, with a cube area density of 0.25, and aspect ratio of 1. Numerical integration was done over 12 hours for a domain size of 64H x 64H x 8H, with a 1.5-m grid resolution. In spite of equal horizontal-averaged heat flux for all cases, the momentum flux differs per position of heated surface. The proximity, orientation, and horizontal projection of heating for each urban surface factor into momentum and heat exchange. Canyon surfaces have stronger canopy mixing, parallel surfaces faster mean winds and inward turbulent exchange, and horizontal surfaces larger turbulence statistics near their proximity. The model agrees with previous studies, and illustrated mechanism-driven differences between momentum and heat transfers.

Key Words **:** *Bulk transfer coefficients, surface heat flux, Large-Eddy Simulation, urban street canyon*

1. INTRODUCTION

Ventilation of urban heat islands is a major motivation for studies involving bulk transfer coefficients of urban surfaces using field measurements[1),2),3)], wind tunnel experiments[3),4),5)], and computational fluid dynamics (CFD) models[3)]. Dependence of bulk coefficients on numerous variables complicates comparative analyses for outdoor and wind tunnel experiments. Numerical simulation, specifically Large Eddy Simulation (LES), has the advantage of normalizing extraneous variables to enable focus on the turbulent effects of a single determining factor, and it does this for a three-dimensional (3D), sufficiently large domain with fine spatial and temporal resolutions.

Although field measurements provide vital information from real cities and are used to validate models, obtaining comprehensive turbulence statistics is encumbered by variable outdoor settings and spatially limited field instrumentation[1),2),3)]. Parameters and measurements are more manageable in wind tunnel experiments, yet, results of such scale models are inherently dependent on scale, fetch, reference height, dimensionality, methodology, and the assumed heat-mass transfer analogy[3),4),5)]. Due to the varied settings of previous studies, a complete understanding of heat ventilation of urban surfaces across a comprehensive range of urban geometries, flow regimes, thermal stabilities and domain scales, is yet to be attained[1)]. Heat flux coefficients of CFD studies[3)] closely approximated mass transfer coefficients of wind-tunnel results[4)], but are limited to two-dimensional experiments.

Previous studies[1,)2),3),4),5)] have called for simultaneous 3D turbulence measurements within and above urban-like roughness of sufficient fetch with other variables held constant. The dimensionality, fine temporal and spatial resolutions of the model used in this study, agree mostly with previous studies, and reveal evidence of mechanism-driven differences between momentum transfer and heat transfer, wherein the former is influenced more by turbulence intensity and pressure fluctuation, and the latter by vertical temperature gradient and heat ventilation efficiency.

2. OBJECTIVE

The purpose of the study is to evaluate the effect of a heated urban surface on heat ventilation of a 3D array of urban-like roughness by numerically computing for bulk transfer coefficients for momentum and heat fluxes. Constant heat flux is applied for each surface, whose position is relative to the mean wind direction – roof, ground, and windward wall, leeward wall, and streamwise wall.

3. METHODOLOGY

Using Parallelized LES Model (PALM)[6], a 1 m/s wind is simulated over explicitly resolved cube arrays[7] with a size of 24 m along one side, with numerical domain size of 2048 x 2048 x 128 grids and a resolution of 1.5 m/grid. Aspect ratio (cube height per canyon width, H/W) of 1, and heat flux of 0.1 K m/s is applied for each surface, half of this for streamwise wall, and 1/3 for ground. Integration time is set at 12 hours, since quasi-steady flow is attained at a maximum of 10 hours. Developed for massively parallel computers with distributed memory and the Message-Passing-Standard MPI[6], PALM is based on filtered, non-hydrostatic, incompressible Boussinesq form of the Navier-Stokes equations (N-S) Eq. (1), continuity equation Eq. (2), 1st law of thermodynamics Eq. (3), and equation for scalar conservation Eq. (4).

$$\frac{\partial \overline{u}_i}{\partial t} = -\frac{\partial \overline{u}_k \overline{u}_i}{\partial x_k} - \frac{1}{\rho_0}\frac{\partial \overline{p^*}}{\partial x_i} - (\varepsilon_{ijk} f_j \overline{u}_k - \varepsilon_{3jk} f_3 u_{gk}) + g\frac{\overline{\theta^*}}{\theta}\delta_3 - \frac{\partial \tau_{ki}}{\partial x_k} \quad (1)$$

$$\frac{\partial \overline{u}_i}{\partial x_i} = 0 \quad (2)$$

$$\frac{\partial \overline{\theta}}{\partial t} = -\frac{\partial \overline{u}_k \overline{\theta}}{\partial x_k} - \frac{\partial \overline{u_k''\theta''}}{\partial x_k} \quad (3)$$

$$\frac{\partial \overline{s}}{\partial t} = -\frac{\partial \overline{u}_k \overline{s}}{\partial x_k} - \frac{\partial \overline{u_k''s''}}{\partial x_k} \quad (4)$$

where indices $i,j,k \in [1,2,3]$, u_i are the three velocity components (u,v,w), x_i (or x,y,z) the corresponding directions in space, t time, p the air pressure, ρ_0 the air density, θ the potential temperature, s any passive scalar, and $\tau_{ki}(= \overline{u_k''u_i''})$, $\overline{u_k''\theta''}$, and $\overline{u_k''s''}$ are the subgrid-scale (SGS) stresses for momentum, heat and passive scalars. The 4th & 5th terms in Eq. (1) represent the Coriolis effect. Boussinesq approximation neglects density variations except in the buoyancy term[6], and filtering decomposes each N-S parameter into a slowly varying average $\overline{\psi}$ (resolved scale) and a rapidly varying turbulent fluctuation ψ'' (SGS), both of which are spatially averaged over grid volumes at time t:

$$\psi = \overline{\psi} + \psi'' \quad (5)$$

$$\overline{\phi\psi} = \overline{\phi}\,\overline{\psi} + \overline{\phi''\psi''} \quad (6)$$

where ϕ is a secondary atmospheric variable. Deardorff-modified Smagorinsky Model[6] is used to solve for SGS turbulence:

$$\overline{u_k''u_i''} = -K_m\left(\frac{\partial \overline{u}_i}{\partial x_k} + \frac{\partial \overline{u}_k}{\partial x_i}\right) \quad (7)$$

$$\overline{u_k''\theta''} = -K_h\frac{\partial \overline{\theta}}{\partial x_k} \quad (8)$$

$$\overline{u_k''s''} = -K_s\frac{\partial \overline{s}}{\partial x_k} \quad (9)$$

The turbulent diffusion coefficients for momentum, heat and scalars (K_m, K_h and K_s) are parameterized by SGS turbulent kinetic energy (SGS-TKE):

$$\overline{e} = \tfrac{1}{2}\overline{u_i''u_i''} \quad (10)$$

$$K_m = c_m l\sqrt{\overline{e}} \quad (11)$$

$$K_h = K_s = \left(1 + \frac{2l}{\Delta}\right)K_m \quad (12)$$

The Smagorinsky constant c_m = 0.1, characteristic grid length $\Delta = \sqrt[3]{\Delta x \cdot \Delta y \cdot \Delta z}$ and mixing length l is:

$$l = \min\left(\Delta, 0.7d, 0.76\sqrt{\overline{e}}\left(\frac{g}{\theta_0}\frac{\partial \overline{\theta}}{\partial z}\right)^{-1/2}\right) \text{ stable} \quad (13)$$

$$l = \min(\Delta, 0.7d) \quad \text{otherwise} \quad (14)$$

where d is the normal distance to the nearest solid surface. The following prognostic equation and parameterizations solve the SGS-TKE:

$$\frac{\partial \overline{e}}{\partial t} = -\frac{\partial \overline{u}_j \overline{e}}{\partial x_j} - \tau_{ij}\frac{\partial \overline{u}_i}{\partial x_j} + \frac{g\overline{u_3''\theta''}}{\theta_0} - \frac{\partial}{\partial x_j}\overline{\left\{u_j''\left(e + \frac{p''}{\rho_0}\right)\right\}} - \varepsilon \quad (15)$$

$$\overline{u_j''\left(e + \frac{p''}{\rho_0}\right)} = -2K_m\frac{\partial \overline{e}}{\partial x_j} \quad (16)$$

$$\varepsilon = \left(0.19 + 0.74\frac{l}{\Delta}\right)\cdot\frac{\overline{e}^{\frac{3}{2}}}{l} \quad (17)$$

The Temperton algorithm for Fast Fourier Transform[6] is used to solve the Poisson equation for pressure. Boundary conditions include: zero initial velocity gradient and temperature gradient, cyclic condition for the laterals, non-slip condition for the bottom, and slip condition for the top. Turbulence statistics of the final 2 hours are used.

4. RESULTS & DISCUSSION

The bulk transfer coefficients for momentum and heat involve turbulence statistics, such as Reynolds shear stress, streamwise velocity, heat flux, and temperature gradients, all of which are horizontally and temporally averaged, unless otherwise mentioned.

(1) Bulk coefficient for momentum flux

The bulk coefficient (C_d) for momentum flux (τ) is given as

$$C_d = \tau\rho/u^2 \qquad (18)$$

where ρ and u have the units (kg/m^3) and (m/s), respectively.

a) Streamwise wind velocity

Surfaces heated within the canyon have stronger canopy streamwise winds, while surfaces parallel to the streamwise wind have weaker canopy winds but greater velocities above the canopy (**Fig. 1**). Thus, the proximity and orientation of heated surfaces determine the location and magnitude of the bolstered streamwise wind. Hence, ground heating is the median case within and above the canopy. Roof case streamwise velocity profile distinctly increases from a small canyon flow to a relatively fast wind above the canopy. Horizontal surface heating has a larger impact on the mean wind above the canopy due to the larger horizontal projection of heat.

b) Momentum flux

In spite of the fact that all cases have equal horizontal-averaged heat flux, the resulting momentum fluxes are different as per position of surface heating. Heating an urban surface increases the momentum flux by about 8-10 times (**Fig. 2**). Within the canyon, momentum flux profiles follow the general effect of proximity and orientation as for streamwise velocity. Such pattern is not analogous above the canopy, since momentum flux is determined by the proximity of heating, mostly within the canopy. The roof case is an exception since it is above the canopy. The streamwise wall case illustrates that a heated parallel vertical wall has the least momentum resistance due to its orientation and small horizontal projection of its heating. In contrast, the roof case has the largest Reynolds shear stress above the canopy, followed by the windward and leeward walls. The horizontal surfaces have the largest momentum fluxes near their proximity.

c) Canyon center flow field and momentum flux

The intensity of the canyon center vortex (**Fig. 3**) is dependent on the location of the heated surface since rising warm air increases the turbulence near its proximity. Canyon surfaces have the strongest flow fields, and the largest streamwise velocities and momentum fluxes within the canopy. The ground case momentum exchange is the least at the roof level since it is the farthest surface from the roof. Peak values for momentum fluxes are right above the roof-level and near the downstream wall, where velocity gradient and flow convergence are maximum.

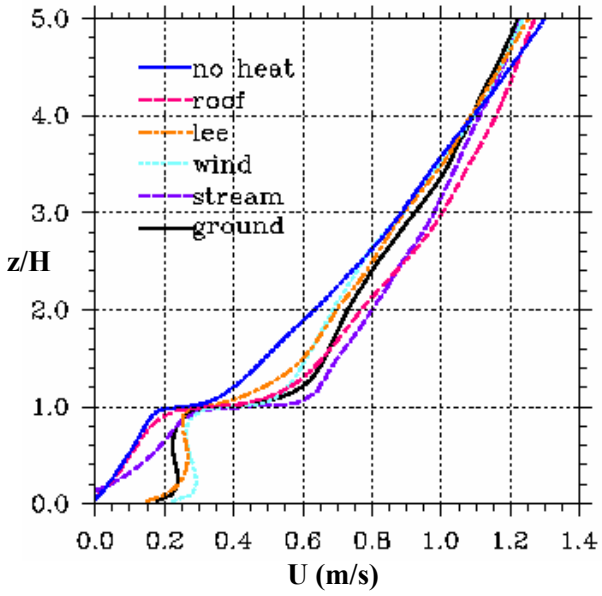

Fig. 1 Streamwise wind velocity.

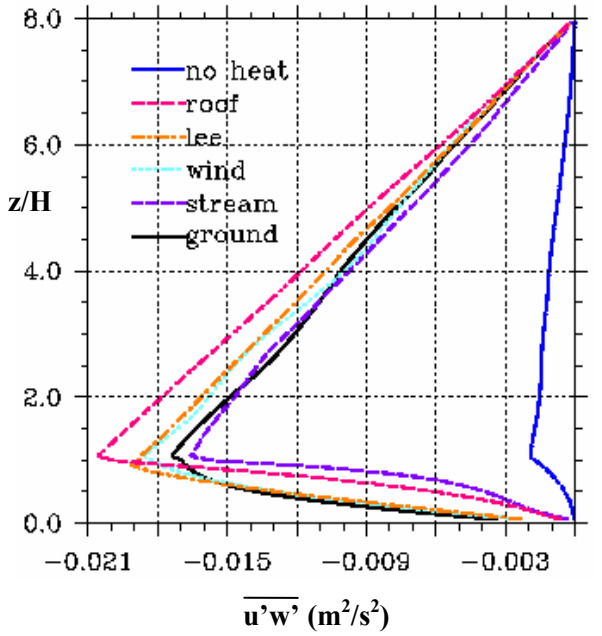

Fig. 2 Total momentum flux.

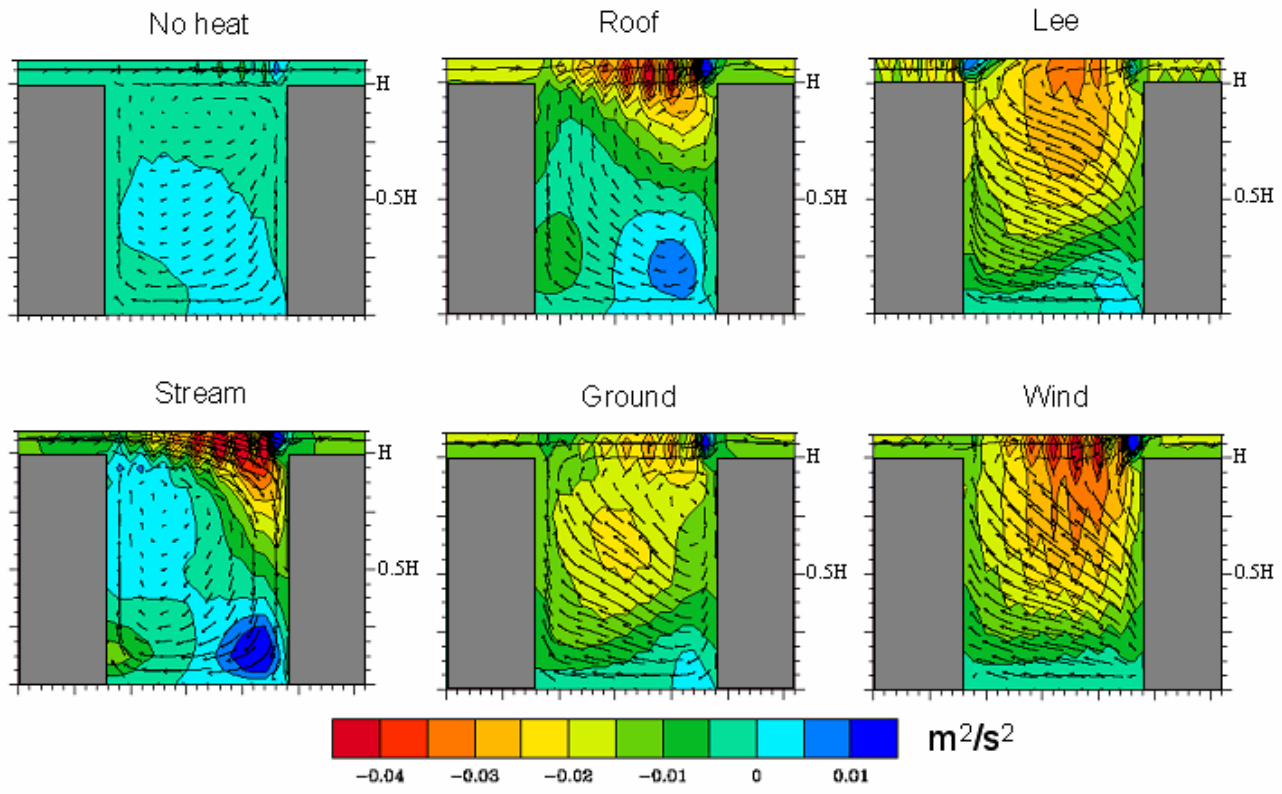

Fig. 3 Contours of span-averaged momentum flux with vector field of the flow field (u and w) within the canyon center.

The heat-induced turbulence right at the roof-level makes the roof case one with the maximum momentum flux. Similarly, rising warm air from the windward wall increases the momentum flux right above the downstream wall. However, heating the leeward wall shifts the peak momentum flux towards the upstream wall.

d) Velocity fluctuations

Spatial fluctuations for streamwise and vertical velocities have opposite patterns (**Figs. 4** & **5**), with canyon surfaces having larger streamwise velocity fluctuations, and parallel surfaces having larger vertical velocity fluctuations. Streamwise statistics have better correlation with momentum flux profiles relative to vertical velocity fluctuations, since streamwise velocity fluctuations within the canopy are larger than vertical velocity fluctuations. Horizontal surfaces have the largest streamwise and vertical velocity fluctuations near their proximity, consistent with their momentum fluxes.

e) Momentum transfer coefficients

Bulk momentum transfer coefficients (**Fig. 6**), are based on the momentum flux and streamwise velocity at 2H. In spite of equal horizontal-averaged heat flux, momentum coefficients are different depending on the position of surface heating. The pattern for the bulk coefficients follows that for the momentum flux.

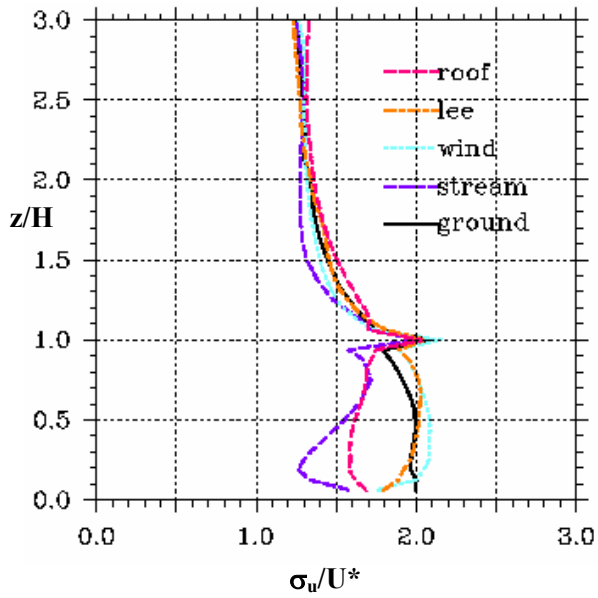

Fig. 4 Standard deviation of streamwise velocity, normalized by u*.

(2) Coefficients for heat flux

The bulk coefficient (C_h) for heat flux ($H/\rho c_p$) is given as

$$C_h = (H/\rho c_p)/u(\theta-\theta_0) \qquad (19)$$

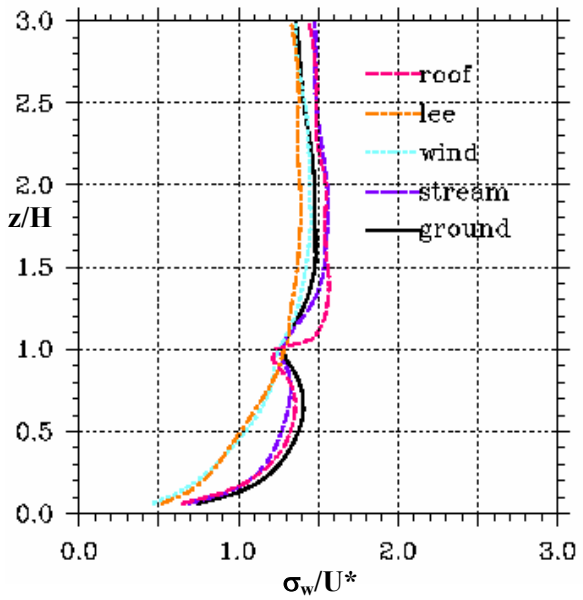

Fig. 5 Standard deviation of vertical velocity, normalized by u*.

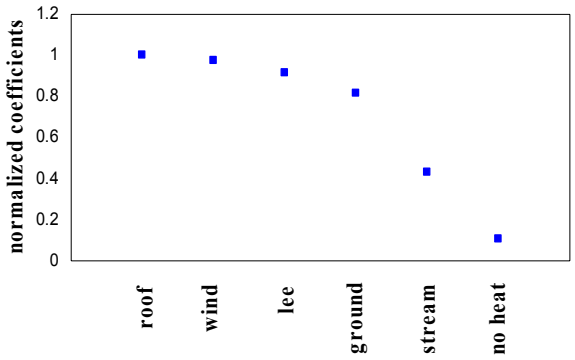

Fig. 6 Bulk transfer coefficients (Cd) for momentum flux normalized by the largest value (roof for Cd)

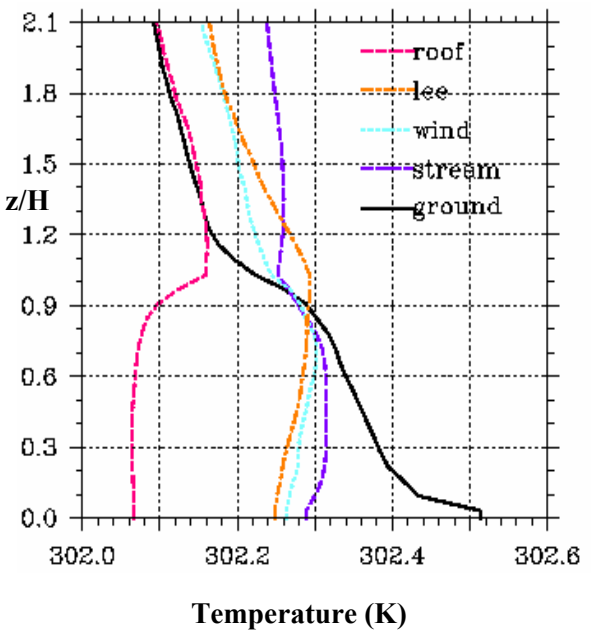

Fig. 7 Vertical profile of potential temperature at the canyon center.

where c_p and θ-θ_0 are the specific heat (m^2/s^2 K), and the difference in potential temperature between a reference and the air (K). Heat flux for the first grid space from any surface is modeled in PALM as perpendicular to the surface, following the Monin-Obukhov Similarity Theory[6].

a) Temperature

From the vertical profiles of temperature in the canyon center (**Fig. 7**), ground heating has the highest temperature in the canyon, followed by vertical walls, since heat is trapped at the canyon. At the roof level, the ground case has the steepest temperature gradient in the canyon, and the roof case right above the building. The former is due to the trapped heat within the canyon and minimal effect of ground heating on the temperature above, while the latter is due to the efficient heat ventilation of the roof.

b) Temperature fluctuations

Temperature fluctuations (**Fig. 8**) have similarities with momentum fluxes and streamwise velocity fluctuations. Vertical walls, having the larger temperatures above the canopy, follow the roof case, which has the largest temperature statistics at the roof-level. Efficient outward heat flux is expected for the roof and vertical walls, and relatively inefficient for the ground case.

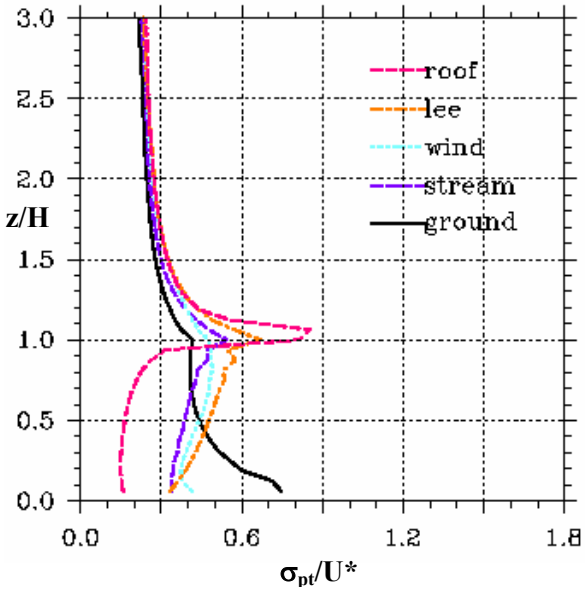

Fig. 8 Standard deviation of potential temperature, normalized by T*.

c) Heat transfer coefficients

The coefficients for heat transfer (**Fig. 9**), are based on heat flux and streamwise velocity at 2H, and difference between the canyon temperature and that at 2H. The order of the coefficients for heat transfer almost agree well with those for momentum.

The exception is that the ground case has larger momentum transfer coefficient, while the streamwise wall has larger heat transfer coefficient, since the former has stronger canyon mixing and higher temperature difference, and the latter has less momentum resistance but more efficient heat ventilation due to its orientation with the streamwise wind. This illustrates the difference between momentum and heat transfer coefficients, wherein pressure fluctuations transport only momentum. Pressure fluctuations must be greater for the ground, while the orientation of the streamwise wall make it more efficient for heat ventilation. The bulk coefficients mostly agree with wind tunnel experiments[4),5)] with a slight difference, wherein the mass transfer coefficients of the leeward wall are smaller than those for the ground[4)] and the streamwise wall[5)]. Wind tunnel experiments assume heat-mass transfer analogy, which is true for fully turbulent flows. The disparity between their results were attributed to the difference in the molecular diffusions of naphthalene and water, wherein the former has larger mass diffusion, while the latter, larger latent heat of evaporation. The fundamental difference between heat and mass is that only heat, as an active scalar, affects the flow field. The transfer coefficient's dependence on wind speed relies on the latter's magnitude, the former sometimes becoming almost constant for large reference velocities at higher elevations for the scale models (7-10H). The reference height (2H) was chosen since the bulk transfer coefficients at the surface layer is of interest, wherein the assumptions of horizontal homogeneity and maximum turbulent fluxes are satisfied.

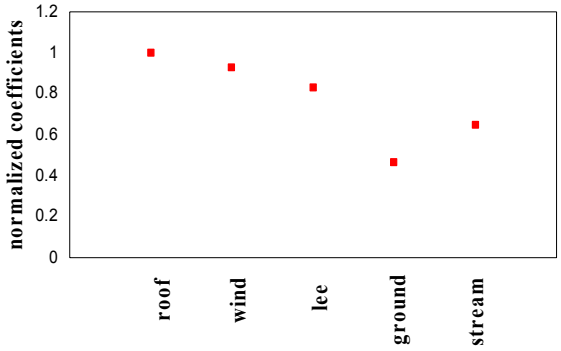

Fig. 9 Bulk transfer coefficients (Ch) for heat flux normalized by the largest value (roof for Ch)

5. CONCLUSION

Bulk transfer coefficients for momentum and heat were numerically computed using LES. The following are the key points revealed from this study:

(1) In spite of equal horizontal-averaged heat flux for all cases, the resulting momentum fluxes are different for each position of surface heating,

(2) bulk transfer coefficients for momentum and heat fluxes are in agreement with each other (**Figs. 6** & **9**) and with previous studies, except for ground and streamwise wall,

(3) which may be explained by the more significant role of turbulence intensity and pressure fluctuation for momentum flux, and vertical temperature gradient and ventilation efficiency for heat flux,

(4) canyon surfaces have the most turbulent mixing within the canopy, parallel surfaces the largest wind velocities above the canopy, and horizontal surfaces the largest turbulence statistics near their proximity.

ACKNOWLEDGMENT: We would like to express our gratitude to the Institute of Meteorology and Climatology, Leibniz University of Hannover, for their support in using PALM.

REFERENCES

1) Hagishima, A., Tanimoto, J., and Narita, K.: Intercomparisons of experimental convective heat Transfer coefficients and mass transfer coefficients of urban surfaces, *Boundary-Layer Meteorol.*, Vol.117, pp.551-576, 2005.

2) Offerle, B., Eliasson, I., Grimmond, C. S. B., Holmer, B.: Surface heating in relation to air temperature, wind and turbulence in an urban street canyon, *Boundary-Layer Meteorol.*, Vol.122, pp.273-292, 2007.

3) Solazzo, E., and Britter, R. E.: Transfer processes in a simulated urban street canyon, *Boundary-Layer Meteorol,.* Vol.124, pp.43-60, 2007.

4) Barlow, J. F., Harman, I. N., and Belcher, S. E.: Scalar Fluxes from urban street canyons. part I: laboratory simulation, *Boundary-Layer Meteorol.*, Vol.113, pp.369-385, 2004.

5) Narita, K.: Experimental study of the transfer velocity for urban surfaces with a water evaporation method, *Boundary-Layer Meteorol.*, Vol.122, pp.293-320, 2007.

6) Letzel, M. O., Krane, M., and Raasch, S.: High resolution urban large-eddy simulation studies from street canyon to neighbourhood scale, *Atmospheric Environment*, Vol.42, pp.8770-8784, 2008.

7) Kanda, M., Moriwaki, R., and Kasamatsu, F.: Large-eddy simulation of turbulent organized structures within and above explicitly resolved cube arrays, *Boundary-Layer Meteorol.*, Vol.112, pp.343-368, 2004.

8) Shaw, R. H., Tavangar J., and Ward, D. P.: Structure of Reynolds stress in a canopy, *J. Climate and Appl. Meteorol.*, Vol.22, pp.1922-1931, 1983.

9) Coceal, O., Thomas, T. G., and Belcher, S.: Spatial variability of flow statistics within regular building arrays, *Boundary-Layer Meteorol.*, Vol.125, pp.537-552, 2007.

(Received September 30, 2008)